Prediction of Meander Delay System Parameters for Internet-of-Things Devices Using Pareto-Optimal Artificial Neural Network and Multiple Linear Regression

DARIUS PLONIS[1], (Member, IEEE), ANDRIUS KATKEVIČIUS[1], (Member, IEEE), ANTANAS GURSKAS[1], VYTAUTAS URBANAVIČIUS[1], (Senior Member, IEEE), RYTIS MASKELIŪNAS[2], AND ROBERTAS DAMAŠEVIČIUS[3]

[1]Faculty of Electronics, Department of Electronic Systems, Vilnius Gediminas Technical University, Vilnius 10221, Lithuania
[2]Kaunas University of Technology, Kaunas 44249, Lithuania
[3]Faculty of Applied Mathematics, Silesian University of Technology, 44-100 Gliwice, Poland

Corresponding author: Robertas Damaševičius (robertas.damasevicius@polsl.pl)

ABSTRACT Meander structures are highly relevant in the Internet-of-Things (IoT) communication systems, their miniaturization remains as one of the key design issues. Meander structures allow to decrease the size of the IoT device, while maintaining the same operating parameters of the IoT device. Meander structures can also work as the delay systems, which can be used for the delay and synchronization of signals in IoT devices. The design procedure of the meander delay systems is time-consuming and cumbersome because of the complexity of the numerical and analytical methods employed during the design process. New methods, which will accelerate the synthesis procedure of the meander delay systems, should be investigated. This is especially relevant when the procedure of synthesis must be repeated many times until the appropriate configuration of the IoT device is found. We present the procedure of synthesis of the meander delay system using the Pareto-optimal multilayer perceptron network and multiple linear regression model with the M5 descriptor. The prediction results are compared with results, which were obtained using the commercial Sonnet© software package and with the results of physical experiment. The difference between the experimentally achieved and predicted results did not exceed 1.53 %. Moreover, the prediction of parameters of the meander delay system allowed to speed up the procedure of synthesis multiple times from hours to only 2.3 s.

INDEX TERMS Antenna arrays, antenna measurements, artificial neural networks, Internet of Things.

I. INTRODUCTION

Internet of things (IoT) is a world-wide network that provides many new possibilities for data acquisition and big data transfer without needing for human interaction. However, the rise of IoT also opens new challenges in the network layer of communications. Because of big amount of data that it is necessary to transfer, researchers try to find algorithms for minimizing the amount of the information without affecting the efficiency of the IoT system [1]. Wireless devices including an antenna and the Radio Frequency (RF) front-end circuits are another big challenges for IoT development [2]. Compact and energy-efficient antennas are vital for future

The associate editor coordinating the review of this manuscript and approving it for publication was Mohsen Khalily[ID].

IoT wireless communication systems [3], [4] and also for energy harvesting systems [5].

It is very important to have reconfigurable antennas, which work in several frequencies used for IoT. For example, there are four desired resonant 0.915/2.45/3.5/5.8 GHz frequencies, which are obtained by an L-shape radiation element [6]. The antenna has a compact size, which is equal to 15.9×25 mm^2. The design of a small dual-band antenna for the IoT based geolocation is presented in [7]. The antenna geometry is based on a folded inverted F antenna, which occupies the top section of a 40×25 mm^2 printed circuit board (PCB).

Nowadays antenna miniaturization, while maintaining the same antennas characteristics, becomes one of the research focuses. Using the meander structures is one of the best
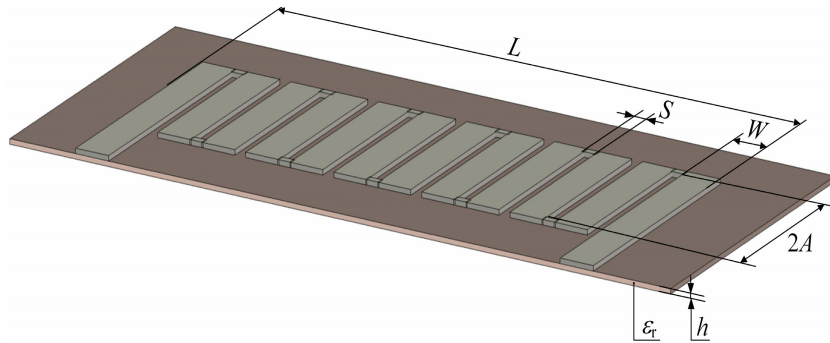
FIGURE 1. The model of the meander delay system, where h is the thickness of dielectric substrate; W is the width of the meander conductor; 2A is the length of the conductor; S is the gap between adjacent conductors; L is the length of the meander delay system; ε_r is the permittivity of the dielectric substrate.

solutions in solving the miniaturization task of microwave devices while maintaining other parameters. Authors of [8] have designed the 3D microstrip meander line antenna that is operating at 2.45GHz for the IoT environment. The size of the antenna was reduced by 1/30λ when compared with original antenna and was equal to 4.3 mm x 4.3 mm. The printed inverted-F 2.4 GHz resonant frequency antenna is presented in [9]. Authors of [10] presented the miniaturized UHF band RFID tag antenna for drug expiration detection that can be attached to the drip chamber in the hospitals. The dipole antenna was downsized by using the meander structure. [11] presented the quad-band monopole planar antenna, which consists of four branches with meander structures in order to operate at different frequency bands for Global Positioning System (GPS), Long Term Evolution (LTE), Worldwide Interoperability for Microwave Access (WiMAX) and wireless LAN (WLAN) in wireless IoT applications. In another example, the antenna is composed of a planar monopole and a planar meander line [12]. The meander structures have allowed to decrease the size of the antennas by keeping the same parameters in all previous examples. Meander structures are used not only in the antennas, but in all microwave devices for shrinking the size of system on package (SoP). [13] have proposed a unique noise suppressing pinwheel meander perforated plane structure in order to mitigate the noise coupling within SoPs. Meander structures are also used to change the radiation pattern of the antenna array [14], to shift the electrical signals in time in order to create a positive feedback in oscillators [15] or to delay and synchronize signals from different sources [16].

The synthesis of the meander delay systems (the computation of constructional parameters of the line in accordance with its predetermined electrical characteristics) is a difficult and time-consuming operation [17]. The mathematical model should be adjusted for every different meander delay structure using analytical methods. It requires specific knowledge and a lot of time [18]. The design procedure using the numerical methods (such as the method of moments, finite-difference time-domain method) is more universal, but the computation time using the numerical methods can last hours or even days [19]. Time becomes a problem especially when

even approximate constructive parameters are not known and calculations have to be repeated many times. Therefore, researchers try to find new methods for modeling of microwave devices.

One of the options available are artificial neural networks (ANN). ANN allows of predicting results very fast after the correct training of the network has been done [20]. There are many examples of the application of ANNs for analysis of microwave devices [21], their synthesis [22] and design [23].

Meander delay system have nonlinear dependencies between constructive and electrical parameters. Therefore, it is difficult to collect the correct data for the training of the neural network and to choose the optimal structure of the network. The synthesis of the meander delay system using multilayer perceptron (MLP) is presented in [24]. The synthesis of hybrid meander delay system also using MLP is presented in [25].

In this paper we present a methodology for the synthesis of the meander delay system. Our contribution is the application of Pareto-optimal MLP to predict results of synthesis of different models of meander delay systems.

II. MATERIALS AND METHODS
A. MODEL OF THE MEANDER DELAY LINE
Meander microstrip delay line (MMDL) favorably distinguished from the variety of electromagnetic lines because their structure satisfies very well the modern technologies of production of microwave devices. The basis of the design of the MMDL (Figure 1) is dielectric substrate, on one side of which the zigzag conductor has formed and on the other side, there is a continuous conductive layer a reference conductor.

The slowdown of signal in the passive lines, created on lumped elements, can be explained by the stretched in time accumulation of energy of the electric or magnetic field respectively in capacitors or inductors. The main drawback of such delay lines (DLs) is a relatively narrow bandwidth. The delay lines with distributed parameters, or electromagnetic DLs tend to have a wide, starting from zero bandwidth. The required delay time in this case is caused by the passage of the signal (electromagnetic wave) of a certain distance,

Algorithm 1 The Synthesis Algorithm of the Microstrip Multiline Delay Lines

---

1. Initially, the desirable electrical parameters of the DLs are known: t_d – the phase delay time, t_{dS}– one-step delay time, Z_0– characteristic impedance, Δf– the bandwidth of the DLs. Then the design parameters of DLs are approximate selected: W – the width of the meander conductor; S – the gap between neighbor conductors; $2A$ – the length of the conductor; L – the length of the DLs; ε_r – the relative permittivity of the dielectric substrate of the DLs; h – the thickness of dielectric substrate; t – the conductive thickness of the meander.
2. Calculation of the characteristic impedance Z_0 of the DLs after the approximate selection of the width W of the meander conductor.
3. **if** The calculated Z_0 is equal to the required Z_0 **then**
    Go to the step 5.
  else
    Go to the step 4.
  end if
4. Update the width $W = W + \Delta W$ of the meander conductor and go back to the step 2.
5. Calculation of the phase delay t_d time of DLs.
6. **if** The calculated t_d is equal to the required t_d **then**
    Go to the step 8.
  else
    Go to the step 7.
  end if
7. Update the length $2A = 2A + \Delta 2A$ of the conductor of the DLs and go back to the step 5.
8. Calculation of the tolerance of the phase delay Δt_d time of DLs.
9. **if** $\Delta t_d \leq t_{d\Delta f}$ **then**
    Go to the step 11.
  else
    Go to the step 10.
  end if
10. Update the length $L = L + \Delta L$ of the DLs and go back to the step 5.
11. Calculation of the one-step delay time t_{dS} of the DLs.
12. **if** The calculated t_{dS} is equal to the required t_{dS}? **then**
    Go to the step 14.
  else
    Go to the step 13.
  end if
13. Update the gap $S = S + \Delta S$ between neighbor conductors of the DLs and go back to the step 2.
14. The end of the algorithm.
Obtained: W, S, $2A$, L. Calculated: $t_d(f)$, $Z_0(f)$, Δf, t_{dS}.

---

usually at a speed less than the speed of light in vacuum. The main disadvantage of the electromagnetic DLs is a relatively small delay time, which is usually not exceeding a few nanoseconds.

B. SYNTHESIS ALGORITHM

The basic algorithm (see Algorithm 1, which will be used together with artificial neural networks) of synthesis of the meander delay lines (MDLs) consists of four cycles. Each cycle ends only when the desired value of the electrical parameter is reached within the permissible variation when a certain design parameter is changed. For example, the required impedance value with an allowable deviation is obtained by changing the width W of the meander conductor in the first cycle of the Algorithm 1 (steps 2–4).

The variation of height $2A$ of the meander produces the required value of the phase delay time in the second cycle of the Algorithm 1 (steps 5–7). The variation of the length of the meander L produces a tolerance for the phase delay time at the highest frequency bandwidth in the third cycle of the Algorithm 1 (steps 1, 8, 9 and 11). However, the length of the meander has an effect on the previously calculated phase delay. Therefore, it returns to the second cycle after the third cycle. The variation of the width of the gap S between the adjacent meander rows results in a required value of the one-step delay time in the fourth cycle of the Algorithm 1 (steps 1, 10, 12 and 14). Calculations returns to the first cycle of the algorithm every time the width S changes, since the width of the gap affects all electrical parameters of the meander DLs.

All constructive parameters and electrical characteristics of the meander DLs are returned after the step value of the phase delay time is obtained in the step 14 of the Algorithm 1. It is important that the step value of the phase delay time should not exceed the permissible deviation. The design of the meander DL is based on the design of the microstrip delay line the cross-sectional parameters of which correspond to the design parameters of the meander DL in this algorithm. All expressions of the computation are basically based on capacitances per unit length C_{1e} and C_{1o} of DLs. The subscript indices "e" and "o" in this case denote the even and odd multiplication of the line, accordingly. The capacitances per unit length can be calculated in various ways. The discussion of mathematical formulas for calculation separate electrical parameters is presented in the following subsections.

C. CALCULATION OF THE CHARACTERISTIC IMPEDANCE IN LOW FREQUENCIES OF DLS

The calculation of the characteristic impedance in low frequencies of DLs is performed in steps 2 – 4 of the Algorithm 1.

The characteristic impedance in the low frequency can be represented by the formula

$$Z_{LF} = Z_0 = \sqrt{\frac{1}{Y_e Y_o} \sqrt{\frac{\varepsilon_{refo}}{\varepsilon_{refe}}}}, \tag{1}$$

here Y_e and Y_o are the conductivities of waves (index e means the even excitation) and (index o means the odd excitation), respectively; ε_{refe} and ε_{refo} are the relative DL effective permitivities. The wavelengths and effective dielectric permitivities are calculated from DLs of C_1, $C_{1e}^{(a)}$, C_{1o} and C_{1o} (a),

in which the index (a) indicates that the dielectric basis is replaced by the air in the line. So:

$$Y_e = c_0\sqrt{C_{1e}C_{1e}^{(a)}}, \tag{2}$$

$$Y_o = c_0\sqrt{C_{1o}C_{1o}^{(a)}}, \tag{3}$$

$$\varepsilon_{\mathrm{refe}} = \frac{C_{1e}}{C_{1e}^{(a)}}, \tag{4}$$

$$\varepsilon_{\mathrm{refo}} = \frac{C_{1o}}{C_{1o}^{(a)}}, \tag{5}$$

$$C_{1e} = C_p + 2C_f, \tag{6}$$

$$C_{1e}^{(a)} = C_p^{(a)} + 2C_f^{(a)}, \tag{7}$$

$$C_{1o} = C_p + 2\left(C_{gd} + C_{ga}\right), \tag{8}$$

$$C_{1o}^{(a)} = C_p^{(a)} + 2\left(C_{gd}^{(a)} + C_{ga}^{(a)}\right), \tag{9}$$

where c_0 is the light speed in vacuum; C_p is the partial volume capacitor consisting of a DL microstrip, dielectric base and full screen; C_f is the DL edge of the microstrip, which measures the distribution of the electric field in the space between the microstrips; C_{gd} and C_{ga} are the interconnections between the adjacent DL microstrips in the case of uneven excitation of DL through the dielectric substrate and air, respectively.

Note that C_g, C_{gd} and C_{gas} are calculated using the conformal exchange method and empirical expressions:

$$C_p = \varepsilon_0\varepsilon_r\frac{W}{h}, \tag{10}$$

$$C_f = \frac{C_{f1}}{1 + A \cdot Sh\tanh\left(10S/h\right)}\sqrt{\frac{\varepsilon_r}{\varepsilon_{\mathrm{ref1}}}}, \tag{11}$$

where

$$C_{f1} = \frac{\sqrt{\varepsilon_{\mathrm{ref1}}}}{2c_0Z_{01}} - \frac{C_p}{2}, \tag{12}$$

where S is the singular length of the edge of the microstrip line; Z_{01} is the characteristic impedance of this line and $\varepsilon_{\mathrm{ref1}}$ is the relative effective dielectric permittivity.

$$Z_{01} = \frac{\eta}{2\pi\sqrt{\varepsilon_{\mathrm{ref1}}}}\ln\left(\frac{8h}{W} + 0.25\frac{W}{h}\right),$$
$$\text{when } \frac{W}{h} \leq 1, \tag{13a}$$

$$Z_{01} = \frac{\eta}{\sqrt{\varepsilon_{\mathrm{ref1}}}}\left[\frac{W}{h} + 1.393 + 0.667\ln\left(\frac{W}{h} + 1.444\right)\right]^{-1},$$
$$\text{when } \frac{W}{h} > 1, \tag{13b}$$

where $\eta = 120\,\pi = 377\,\Omega$ is vacuum characteristic impedance.

$$\varepsilon_{\mathrm{ref1}} = \frac{\varepsilon_r + 1}{2} + \frac{\varepsilon_r - 1}{2}\frac{1}{\sqrt{1 + 10h/W}}. \tag{14}$$

The size of the expression A (11) is calculated as follows:

$$A = \exp\left[-0.1e^{(2.33-2.53W/h)}\right]. \tag{15}$$

The value of C_{ga} occurs due to the margin field between the microstrip above the dielectric substrate with an odd DL excitation. It is calculated as follows:

$$C_{ga} = \varepsilon_0\frac{K\left(k'\right)}{K\left(k\right)}, \tag{16}$$

$$k = \frac{S/h}{S/h + 2W/h}, \tag{17}$$

$$k' = \sqrt{1 - k^2}, \tag{18}$$

where the ratio of the total functions $K(k)$ and $K(k')$ is determined as follows:

$$\frac{K(k)}{K'(k)} = \left[\frac{1}{\pi}\ln\left(2\frac{1+\sqrt{k'}}{1-\sqrt{k'}}\right)\right]^{-1}, \quad \text{when } 0 \leq k \leq 0.7, \tag{19}$$

$$\frac{K(k)}{K'(k)} = \frac{1}{\pi}\ln\left(2\frac{1+\sqrt{k}}{1-\sqrt{k}}\right), \quad \text{when } 0.7 < k \leq 1.0 \tag{20}$$

where C_{gd} is described in the margin field between the microstrip substrate dielectric in the case of odd excitation and is calculated as follows:

$$C_{gd} = \frac{\varepsilon_0\varepsilon_r}{\pi}\ln\left(\coth\frac{\pi S}{4h}\right) + 0.65C_f\left(\frac{0.02}{S/h}\sqrt{\varepsilon_r} + 1 - \frac{1}{\sqrt{\varepsilon_r}}\right). \tag{21}$$

In case of finite microstrip thickness t, the lengths can be calculated using the concept of effective W_t.

In the case of even excitation:

$$\frac{W_t^{(e)}}{h} = \frac{W}{h} + \frac{\Delta W}{h}\left(1 - 0.5e^{-0.69\Delta W/\Delta t}\right). \tag{22}$$

In the case of odd excitation:

$$\frac{W_t^{(e)}}{h} = \frac{W}{h} + \frac{\Delta W}{h}\left(1 - 0.5e^{-0.69\Delta W/\Delta t}\right), \tag{23}$$

where:

$$\frac{\Delta t}{h} = \frac{1}{\varepsilon_r}\frac{t/h}{S/h}, \tag{24}$$

$$\frac{\Delta W}{h} = \frac{1.25}{\pi}\cdot\frac{t}{h}\left(1 + \ln\frac{4\pi W}{t}\right), \quad \text{when } \frac{W}{h} \leq \frac{1}{2\pi}, \tag{25a}$$

$$\frac{\Delta W}{h} = \frac{1.25}{\pi}\cdot\frac{t}{h}\left(1 + \ln\frac{2h}{t}\right), \quad \text{when } \frac{W}{h} \geq \frac{1}{2\pi}. \tag{25b}$$

D. CALCULATION OF DELAY TIME OF DLS

The calculation of the delay time of DLs is performed in the steps $5 - 7$ of the Algorithm 1. The nominal (required) delay time is calculated as the time required to squeeze the path L (L is the meander length) by the electromagnetic wave, according to the following formula:

$$t_d = c_0L/k_{d\,\mathrm{LF}}, \tag{26}$$

where L is the length of the meander, which is determined as the whole steps length $(W + S)$ of the meander's number of meander rods (steps):

$$L = (W + S)\cdot(t_d/t_{d\,S}) - S, \tag{27}$$

where k_{dLF} is the low frequency (LF) factor of the synthesized line is calculated as follows:

$$k_{\mathrm{d\,LF}} = \frac{2A}{W+S}\sqrt{\frac{Y_{\mathrm{e}}}{Y_{\mathrm{o}}}}\sqrt{\varepsilon_{\mathrm{refe}}\varepsilon_{\mathrm{refo}}}, \qquad (28)$$

here $2A$ is the height of the meander. The meander height is changed to achieve the nominal delay time (steps 6 and 7 of the synthesis algorithm).

E. CALCULATION OF THE BANDWIDTH OF DLS

The calculation of the bandwidth of DLs is performed in steps 8, 9 and 11 of the Algorithm 1. The width of the meander microstrip DL bandwidth is determined by permissible phase distortion. Phase distortions are considered to be acceptable if the deviation of the phase frequency response characteristics from the straight line does not exceed 0.35 rad. From here we can determine the maximum deviation of the delay time from the nominal value at the highest frequency of the bandwidth:

$$t_{\mathrm{d}\,\Delta f} \le \frac{0.35}{2\pi\,\Delta f}, \qquad (29)$$

where Δf is the nominal bandwidth of the bandwidth.

The tolerance time delay is calculated as the absolute difference between the nominal delay time t_{d} and the delay time at a certain frequency f:

$$t_{\mathrm{d}\,\Delta f} = |t_{\mathrm{d}} - t_{\mathrm{d}}\,(f)|, \qquad (30)$$

For the delay time $t_{\mathrm{d}}(f)$, the dispersion equation is determined (essentially, the dependence $t_{\mathrm{d}}(f)$ is calculated). Next, the widths of the bandwidth are determined by expressions (31) and (32).

The dispersion equation looks like this:

$$D_{\mathrm{c}}D_{\mathrm{n}} = 0, \qquad (31)$$

where

$$D_{\mathrm{c}} = Y\,(\theta)\tan(k_1 A) - Y\,(\theta+\pi)\cot(k_2 A)\cdot\tan^2(\theta/2), \qquad (32)$$

$$D_{\mathrm{n}} = Y\,(\theta)\cot(k_1 A) - Y\,(\theta+\pi)\tan(k_2 A)\cdot\tan^2(\theta/2). \qquad (33)$$

The dispersion equation (31) for a particular frequency f is solved numerically, for example, by a serial approach, by changing the parameter (phase difference between adjacent meander rods (DL conductors)) until a value equal to zero is reached, within the tolerance (e.g. $= 10^{-6}$).

Further we discuss briefly (32) and (33) expressions of sizes. A is the meander height.

$$k_1 = k_0\sqrt{\varepsilon_{\mathrm{ref}}\,(\theta)}, \qquad (34)$$

$$k_2 = k_0\sqrt{\varepsilon_{\mathrm{ref}}\,(\theta+\pi)}, \qquad (35)$$

$$k_0 = \frac{\omega}{c_0} = \frac{2\pi f}{c_0}, \qquad (36)$$

where f is a calculated frequency value.

$$\varepsilon_{\mathrm{ref}}\,(\theta) = \left[\frac{Y_{\mathrm{e}}\cos^2(\theta/2) + Y_{\mathrm{o}}\sin^2(\theta/2)}{Y_{\mathrm{e}}^{(\mathrm{a})}\cos^2(\theta/2) + Y_{\mathrm{o}}^{(\mathrm{a})}\sin^2(\theta/2)}\right]^2, \qquad (37)$$

is a microstrip DL that simulates a meander delay line with a relative effective dielectric penetration when the line is triggered sinphasically (i.e. the difference between adjacent conductors is equal).

$$\varepsilon_{\mathrm{ref}}\,(\theta+\pi) = \left[\frac{Y_{\mathrm{e}}\sin^2(\theta/2) + Y_{\mathrm{o}}\cos^2(\theta/2)}{Y_{\mathrm{e}}^{(\mathrm{a})}\sin^2(\theta/2) + Y_{\mathrm{o}}^{(\mathrm{a})}\cos^2(\theta/2)}\right]^2, \qquad (38)$$

is the relative effective dielectric penetration of a microstrip DL that simulates a meander delay line when the line is excited by an anaphase (i.e., the difference between the adjacent conductor phases is $\theta + \pi$).

Similarly, the waveguides of expressions (37) and (38) are:

$$Y(\theta) = Y_{\mathrm{e}}\cos^2\frac{\theta}{2} + Y_{\mathrm{o}}\sin^2\frac{\theta}{2}, \qquad (39)$$

$$Y(\theta+\pi) = Y_{\mathrm{e}}\sin^2\frac{\theta}{2} + Y_{\mathrm{o}}\cos^2\frac{\theta}{2}. \qquad (40)$$

F. CALCULATION OF DELAY TIME OF ONE STEP

The calculation of the one step delay time of DLs is performed in steps 10, 12 and 14 of the Algorithm 1. Multifaceted DL allows to set the desired delay time by a certain step. The duration of this step is calculated in steps 10, 12 and 14 of the synthesis (Algorithm 1). The length of one step of the meander is initially determined in order to calculate the one-step delay time:

$$t_{\mathrm{d\,S}} = \frac{c_0(W+S)}{k_{\mathrm{d\,LF}}}, \qquad (41)$$

where k_{dLF} is the delay factor for low frequencies, which is calculated from the expression (28).

G. MULTIPLE LINEAR REGRESSION

For this study Multiple Linear Regression (MLR) [26] model with the M5 descriptor selection method and a fixed small ridge parameter 10^{-7} was used. In M5, a MLR model is initially build on all descriptors, and then descriptors with the smallest standardized regression coefficients are step-wisely removed from the model until no improvement is observed in the estimate of the average prediction error given by the Akaike information criterion [27]. Linear regression produces an equation, where the given input variables are presented as independent variables, on which the target variable is dependent upon:

$$y = w_0 + w_1 x_1 + w_2 x_2 + \ldots + w_{\mathrm{n}} x_{\mathrm{n}}. \qquad (42)$$

The training of MLR is implemented by updating the weight vector w in order to minimize the square error $E(w)$ using the gradient descent method, which starts from an initial weight vector $w(0)$, and for every iteration j computes the weight vector difference $\Delta w(j)$ so, that it moves to the direction for which the function $E(w)$ has the greatest rate of decrease. The error is the difference between the predicted value and the observed value, and in our case it is calculated

using the sum of squares of residuals:

$$E(w) = \frac{1}{n} \sum_{i=1}^{n} \left[(w_i x_i + w_0) - y_i \right]^2 + \alpha \sum_{i=0}^{n} [w_i]^2, \quad (43)$$

where $\alpha = 10^{-7}$ is a ridge parameter. To find w such that $E(w)$ is minimized, the gradient descent is used, iteratively updating w:

$$w_i(j+1) = w_i(j) - \partial E(w)/\partial w_i. \quad (44)$$

We repeat above until we reach convergence, i.e. derivative is small and w not changing sufficiently.

H. M5 RULES

The third method used for the classification and prognosis was M5 Rules [28], which generates a decision list for regression problems using separate-and-conquer (see Algorithm 2). In each iteration it builds a model tree using M5 and makes the ''best'' leaf into a rule. This technique is based on model trees by Wang and Witten [29]. A model tree method builds trees, whose leaves are associated with a multivariate linear model.

Algorithm 2 M5 Rules

A. A tree learner (model trees) is applied to the full training set and a pruned tree is learned, maximizing the expected error reduction as a function of the standard deviation of the output parameters.
B. Best leaf is made into a rule and the tree is discarded.
C. All instances covered by the rule are removed from the dataset.
D. A–C steps are repeated until all instances are covered by one or more rules.

The decision, which leaf should be made as a rule (B step) is based on its coverage, i.e. leaf which covers most examples is selected.

I. PARETO OPTIMAL NEURAL NETWORK

For our task, we used a Pareto-optimal neural network constructed using the Pareto-optimal neural network search algorithm presented in [30]. We applied this algorithm to evolve a MLP neural network optimized for efficiency criteria. The approach is an iterative population-based one, which approximates the Pareto front of optimal neural network solutions in a single search process.

A neural network was represented as a Directed Acyclic Graph (DAG) of cells, where each cell is composed of B blocks. Each block is a mapping two input vectors to one output vector and it can be represented by a 4-tuple, (I1;O1; I2;O2), here Ik specifies the input for the operation Ok. The result of the two operations O1 and O2 are summed together and a soft thresholding function is applied to form the output of the block. Unused blocks are concatenated in the depth dimension to form the final output of the cell.

The resulting neural network is trained, using the classical error backpropagation algorithm. MLP's training is implemented by updating the weight vector w in order to minimize the square error $E(w)$ using the gradient descent method, which starts from an initial weight vector $w(0)$, and for every iteration j computes the weight vector difference $\Delta w(j)$ so, that it moves to the direction for which the function $E(w)$ has the greatest rate of decrease. Automatic pre-processing was used to normalize the data between 0 and 1 for each variable. The learning rate and momentum were respectively set at $\eta = 0.3$ and $\alpha = 0.2$.

III. EXPERIMENTAL EVALUATION
A. DATA COLLECTION

The data collection for automatic predictor training was performed by selecting data, which were obtained by the commercial state-of-the-art Sonnet© software package our developed method. The input matrix of the automatic predictor consisted of Z_{LF}, t_d, Δf, ε_r, h parameters. The output matrix of the automatic predictor consisted of W, $2A$, L and S parameters (where measurement unit mm.). The calculated data samples were divided in to training (70% of samples), validation (15% of samples) and testing (15% of samples) data samples.

The size of the input and output matrices of the automatic predictor was equal to 4×189 and 4×189 respectively. 189 data samples were used for training, 35 data samples were used for validation ad 35 data samples were used for testing.

B. PHYSICAL DESIGN AND EVALUATION OF MEANDERS

An experimental model of the meander microstrip delay line was manufactured and investigated to verify the reliability of the proposed methods of synthesis of such lines using artificial neuron networks. The initial conditions for the synthesis of the meander line: the delay time — 4.7 ns, the characteristic impedance — 50 Ω, the relative permittivity (dielectric constant) of the substrate — 7.3 and its thickness 0.5 mm, were set as requirements. The synthesis of the meander line according to the proposed method lasted 2.3 s (CPU Intel-i5, 16 GB RAM). The following design parameters of the meandering microstrip delay line were obtained because of the synthesis: the width of the meander conductor $W = 0.47$ mm, the width of the gap between the conductors $S = 0.48$ mm, the height of the meander $2A = 29.8$ mm, the total length of the meander $L = 16.7$ mm. It is very problematic or even impossible to place such a meander line on a typical ceramic substrate measuring 60 by 48 mm; therefore, an experimental model of the delay line was made on two substrates (Figure 2).

The block diagram of the experimental equipment for measuring the delay time of the meander line is shown in Figure 3 (a), and a general view of the experiment environment is presented in Figure 3 (b). The test pulse generator (the set of the pulse generator mainframe GZ-1106DL2 and pulse shaper GZ1117GN-03) generates pulses with a duration
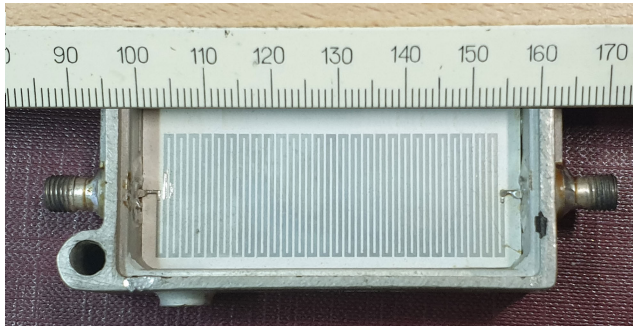
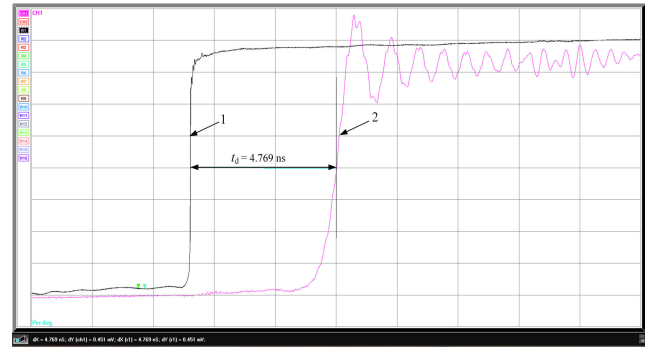**FIGURE 2.** Experimental layout meander microstrip delay line.
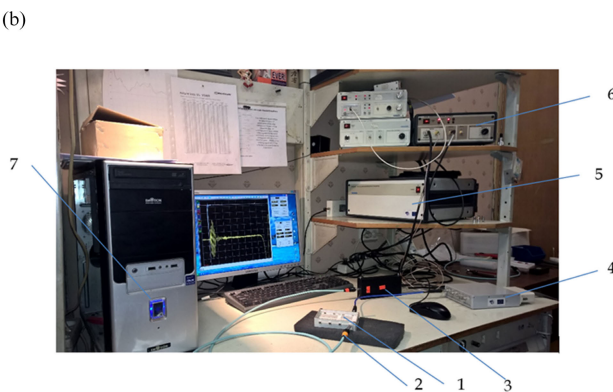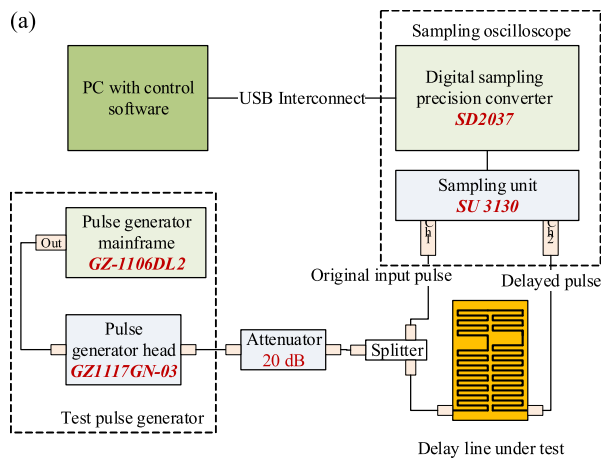
(a)

(b)

FIGURE 3. A block diagram of an experimental measurement of the delay time of a prototype of the meander microstrip line (a), and a general photograph of the experiment (b); where 1 is the meander delay line-under-test, 2 is the attenuator, 3 is the pulse shaper GZ117GN-03, 4 is the sampling unit SU-3130, 5 is the digital sampling precision converter SD20037, 6 is the pulse generator mainframe GZ-1106DL2, 7 is the computer with the control software.

of 3.0 ps and an amplitude of 30 V. However, no more than 1 V voltage can be applied to the input of the sampling unit SU-3130, therefore an attenuator of 20 dB was inserted between the meander line-under-test and the pulse shaper.

The original input and the delayed output pulses of the delay line on the screen of the sampling oscilloscope are shown in Figure 4. Note that the meander line delays the input pulse by 4.769 ns, while expanding it in time. Measured delay time differs less than 1% from the value specified
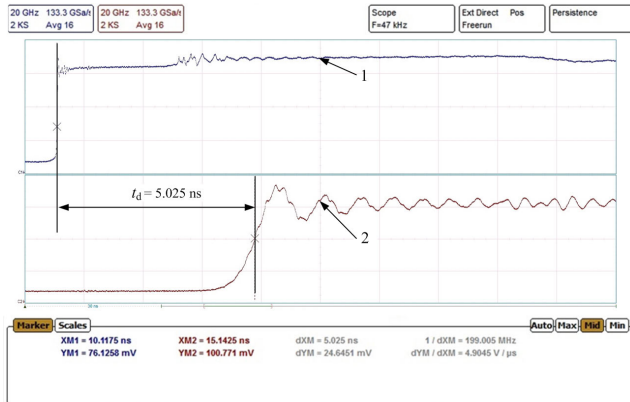

FIGURE 4. An example of signals of input and output pulses of the meander microstrip line, here 1 – pulse at the input of the delay line; 2 – pulse at the output of the delay line, delay time 4.769 ns.

during the synthesis and may be related to the variation of the parameters of the dielectric substrate (its dielectric constant and thickness) and deviations of the dimensions of the meander topology of the line. The expansion of the test pulse after its propagation through the meander delay line is explained by the comparatively narrow bandwidth of the line ($F_{DL} = 0.35$ GHz).

Minor oscillations at the beginning of the output pulse, coinciding in time with the test pulse at the line input were caused by the penetration of the broadband test pulse (its frequency spectrum width is $\sim$2 GHz) from the line input to its output through the substrate dielectric. The frequency of these oscillations is outside the bandwidth of the meander delay line and therefore should not affect its operation.

C. RESULTS
We performed the comparison of the results in three cases (prediction (synthesis) of the design parameters of the meander microstrip delay lines):

Case 1: The meander microstrip delay line, when delay time $t_d = 5.00$ ns, and the characteristic impedance $Z_0 = 50$ Ω, and the relative permittivity ε_r of dielectric substrate is 7.3; the bandwidth $\Delta f = 300$ MHz; the thickness of dielectric substrate $h = 0.5$ mm.

Case 2: The meander microstrip delay line, when delay time $t_d = 4.90$ ns, and the characteristic impedance $Z_0 = 50$ Ω, and the relative permittivity ε_r of dielectric substrate is 7.3; the bandwidth $\Delta f = 300$ MHz; the thickness of dielectric substrate $h = 0.5$ mm.

Case 3: The meander microstrip delay line, when delay time $t_d = 6.20$ ns, and the characteristic impedance $Z_0 = 50$ Ω, and the relative permittivity ε_r of dielectric substrate is 7.3; the bandwidth $\Delta f = 300$ MHz; the thickness of dielectric substrate $h = 0.5$ mm.

The results of the predicted design parameters of the meander microstrip line are presented in Table 1. Note that the measured delay time is 0.025 ns, 0.075 ns and the 0.063 ns higher than these delay times given in the modeling stage (Cases 1–3).

TABLE 1. Predicted/synthesized design parameters of the meander microstrip delay lines.

Case	Predicted design parameters				t_d, ns	Measured t_d, ns
	W, [mm]	$2A$, [mm]	L, [mm]	S, [mm]		
Case 1.	0.476	29.440	20.472	0.476	5.00	5.025
Case 2.	0.474	29.561	19.220	0.362	4.90	4.975
Case 3.	0.495	27.992	35.484	0.540	6.20	6.263

FIGURE 5. An example of signals of input and output pulses of the meander microstrip line, here 1 – pulse at the input of the delay line; 2 – pulse at the output of the delay line, delay time 5.025 ns.

FIGURE 6. An example of signals of input and output pulses of the meander microstrip line, here 1 – pulse at the input of the delay line; 2 – pulse at the output of the delay line, delay time 4.975 ns.

FIGURE 7. An example of signals of input and output pulses of the meander microstrip line, here 1 – pulse at the input of the delay line; 2 – pulse at the output of the delay line, delay time 6.263 ns.

FIGURE 8. Comparison of the calculated and predicted results of parameters of meander microstrip delay lines.

The results of the measurement obtained at different delay times are presented in Figures 5 – 7. The highest difference of the synthesized meander microstrip line is obtained, when the meander microstrip line with $t_d = 4.90$ ns was synthesized and the difference was equal to 1.53 % (Figure 6). The lowest difference of the synthesized meander microstrip line was obtained, when the meander microstrip line with delay time equal to 5.00 ns was synthesized and the difference was equal only to 0.5 % (Figure 5). The characteristic impedance Z_0 and the bandwidth of the meander microstrip lines were not measured during the investigation of the manufactured meander microstrip lines.

The meander microstrip delay line was synthesized using our created algorithm (Algorithm 1) and also designed using the Sonnet© software.

We have compared the prediction results of W, $2A$, L and S parameters. The lowest differences between the calculated and predicted results were obtained at 0 %, when $2A$ parameter is predicted and M5 Rules were used. The highest differences between the calculated and predicted results were obtained, when L parameter of the meander microstrip delay lines is predicted. The prediction error is 115 %, when M5 Rules are not used (see Figure 8). The highest mean error of the prediction is 72.5 %, and lowest mean error of the prediction is 7.68 %, when the M5 Rules are not used. The quality of the automatic predictor can be increased by using M5 Rules. The lowest mean differences between the
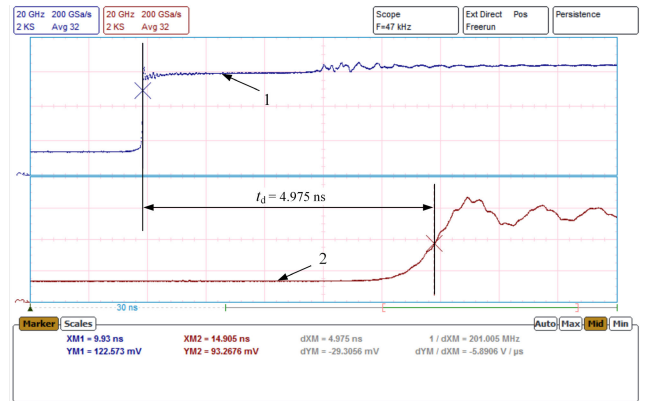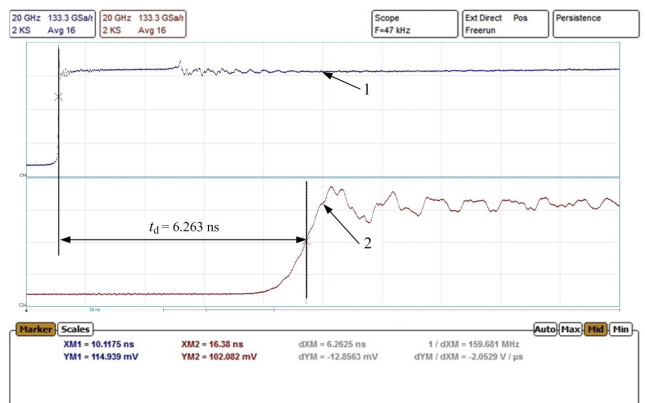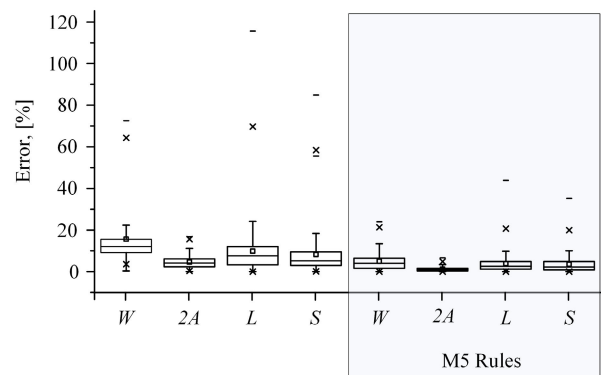
calculated and predicted results were 0.0086 % in this case. The highest mean differences between the calculated and predicted results were 27.5 %.

The analysis of the results shows that it is better to use the automatic predictor with the M5 Rules algorithm (Algorithm 1) for the prediction of design parameters of
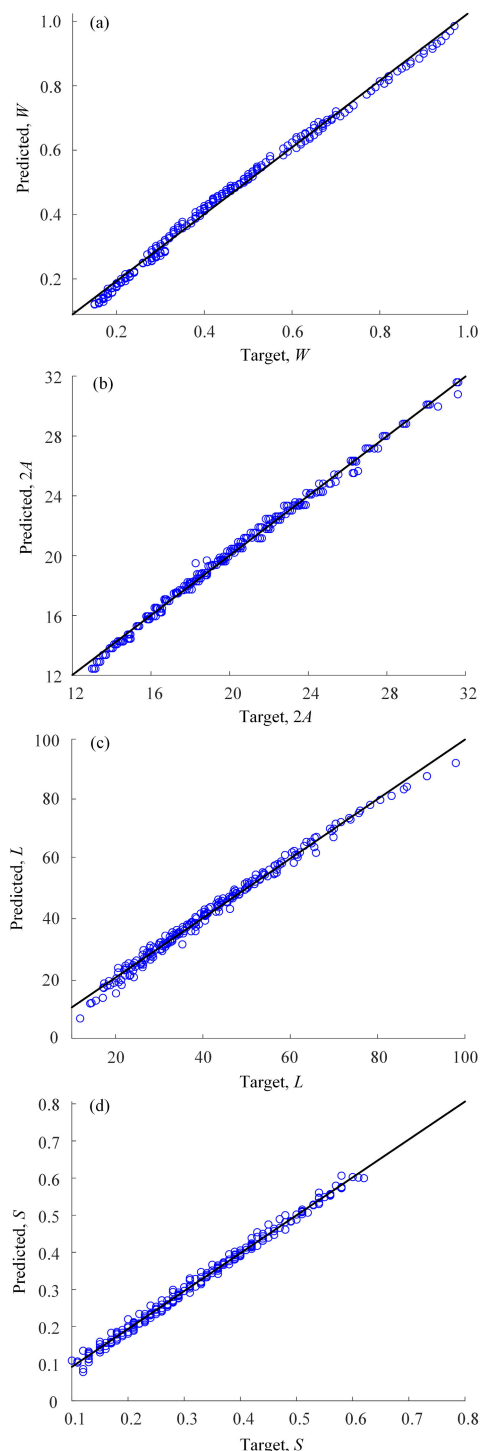
FIGURE 9. Distribution of predicted parameters on target parameters: *W* parameter – (a); *2A* parameter – (b); *L* parameter – (c); *S* parameter – (d).

the meander microstrip delay lines. The error of the prediction is decreased by 2.63 times by using the M5 Rules algorithm. The distribution of the predicted on the target *W*, *2A*, *L* and *S* parameters shows a good linear fit for all values (Figure 9).

IV. CONCLUSION

Positive results of synthesis of meander delay systems were obtained. The prediction using Pareto-optimal neural network and multiple linear regression with M5 descriptor have allowed to shorten the computation time from hours to 2.3 s. Modified structures of the meander delay lines can be investigated in real time when the computation takes only seconds. The *W*, *2A*, *L* and *S* parameters of the meander delay line were predicted. The lowest differences between the calculated and predicted results were received 0 %, when *2A* parameter was predicted and M5 Rules were used. The highest differences between the calculated and predicted results were obtained, when *L* parameter of the meander microstrip delay lines was predicted. The highest mean error of the prediction was 72.5 % and lowest mean error of the prediction was 7.68 % when the M5 Rules were not used.

The highest mean differences between the calculated and predicted results was 27.5 % and the lowest mean differences between the calculated and predicted results was only 0.0086 %, when the M5 predictor the automatic predictor with M5 Rules can be efficiently used for prediction of design parameters of the meander microstrip delay lines. The prediction results were also compared with the results of the physical measurement experiment. The differences between the predicted and measured results did not exceeded 1.53 % in all cases.

REFERENCES

[1] O. Said, A. Elnashar, and O. Elshakankiry, "Optimized mechanism for minimizing data overhead in iot environments: Design, simulation and performance evaluation," *Int. J. Appl. Eng. Res.*, vol. 12, no. 23, pp. 13663–13676, 2017.

[2] K. R. Jha, B. Bukhari, C. Singh, G. Mishra, and S. K. Sharma, "Compact planar multistandard MIMO antenna for IoT applications," *IEEE Trans. Antennas Propag.*, vol. 66, no. 7, pp. 3327–3336, Jul. 2018, doi: 10.1109/tap.2018.2829533.

[3] Q. Awais, H. T. Chattha, M. Jamil, Y. Jin, F. A. Tahir, and M. U. Rehman, "A novel dual ultrawideband CPW-fed printed antenna for Internet of Things (IoT) applications," *Wireless Commun. Mobile Comput.*, vol. 2018, pp. 1–9, Mar. 2018.

[4] Z. Su, K. Klionovski, R. M. Bilal, and A. Shamim, "A dual band additively manufactured 3-d antenna on package with near-isotropic radiation pattern," *IEEE Trans. Antennas Propag.*, vol. 66, no. 7, pp. 3295–3305, Jul. 2018.

[5] W.-S. Chen, C.-M. Cheng, B.-Y. Liao, Y.-L. Chang, and H.-Y. Wang, "Triple-band slot antenna array for energy harvesting for wireless sensor networks," *Sensors Mater.*, vol. 30, no. 3, pp. 587–594, 2018, doi: 10.18494/sam.2018.1827.

[6] Y. Yang, L. Yuanan, and W. Fan, "A compact quad-band monopole antenna for IoT application in WSNs/WLAN/LTE bands," *Adv. Sci. Technol. Lett.*, vol. 123, no. 1, pp. 128–132, 2016, doi: 10.14257/astl.2016.123.25.

[7] L. Lizzi, F. Ferrero, P. Monin, C. Danchesi, and S. Boudaud, "Design of miniature antennas for IoT applications," in *Proc. IEEE 6th Int. Conf. Commun. Electron. (ICCE), Hạ Long Bay, Vietnam* Jul. 2016, pp. 234–237.

[8] A. N. Mohamed, S. N. Azemi, S. A. Suhaimi, and A. A. M. Ezanuddin, "3D miniature antenna design for RFID applications in IoT environment," in *Proc. MATEC Web Conf.*, vol. 97, 2017, pp. 1–7.

[9] C. Y. Cheung, J. S. M. Yuen, and S. W. Y. Mung, "Miniaturized printed inverted-F antenna for Internet of Things: A design on PCB with a meandering line and shorting strip," *Int. J. Antennas Propag.*, vol. 2018, no. 1, 2018, pp. 1–5.

[10] D.-O. Ko and J.-M. Woo, "Design of a small radio frequency identification tag antenna using a corrugated meander line applicable to a drug runout sensor system," *J. Electromagn. Eng. Sci.*, vol. 18, no. 1, pp. 7–12, Jan. 2018.

[11] H. A. Mohamed and K. S. Sultan, "Quad band monopole antenna for IoT applications," *IEEE Int. Symp. Antennas Propag. APS/URSI*, Jul. 2018, pp. 1015–1016.

[12] K. S. Sultan, H. H. Abdullah, and E. A. F. Abdallah, "Low-SAR miniaturized handset antenna using EBG," in *Low-SAR Miniaturized Handset Antenna Using EBG, Itex Open Science*. London, U.K., 2019, ch. 7, pp. 127–147, doi: 10.5772/intechopen.70175.

[13] Y. Han, H. A. Huynh, and S. Kim, "A new pinwheel meander-perforated plane structure for noise suppression in system-on-package," in *Proc. IEEE Electr. Design Adv. Packag. Syst. (EDAPS)*, Honolulu, HI, USA, Dec. 2016, pp. 123–125.

[14] Q. Ma, D. M. W. Leenaerts, and P. G. M. Baltus, "Silicon-based true-time-delay phased-array front-ends at Ka-band," *IEEE Trans. Microw. Theory Techn.*, vol. 63, no. 9, 2015, pp. 2942–2952, doi: 10.1109/tmtt.2015.2458326.

[15] R. Villeneuve, M. Cueille, D. Arnaud-Cormos, J.-F. David, P. Leveque, and A.-J. Durand, "Setup and characterization of a backward wave oscillator delay line scaled down to centimeter- and millimeter-wave ranges," *IEEE Trans. THz Sci. Technol.*, vol. 5, no. 6, pp. 1053–1061, Nov. 2015.

[16] A. Pollakis, L. Wetzel, D. J. Jörg, W. Rave, G. Fettweis, and F. Jülicher, "Synchronization in networks of mutually delay-coupled phase-locked loops," *New J. Phys.*, vol. 16, no. 11, Nov. 2014, Art. no. 113009.

[17] Y. He, G. Wang, and L. Sun, "Direct matrix synthesis approach for narrowband mixed topology filters," *IEEE Microw. Wireless Compon. Lett.*, vol. 26, no. 5, pp. 301–303, May 2016.

[18] S. Staras, R. Martavicius, J. Skudutis, V. Urbanavicius, and V. Daskevicius, *Wide-Band Slow-Wave Systems: Simulation and Application*. Boca Raton, FL, USA: CRC Press, 2012, p. 299.

[19] E. Metlevski, R. Martavicius, A. Katkevičius, D. Plonis, and A. Krukonis, "Parametric synthesis of meander slow-wave system with additional shields," *Acta Phys. Pol. A*, vol. 130, no. 6, pp. 1435–1438, Dec. 2016, doi: 10.12693/aphyspola.130.1435.

[20] J. Zhang, K. Mal, F. Feng, and Q. Zhang, "Parallel gradient-based local search accelerating particle swarm optimization for training microwave neural network models," in *IEEE MTT-S Int. Microw. Symp. Dig.*, Phoenix, AZ, USA, May. 2015, pp. 1–3.

[21] A.-D. Huang, Z. Zhong, W. Wu, and Y.-X. Guo, "An artificial neural network-based electrothermal model for GaN HEMTs with dynamic trapping effects consideration," *IEEE Trans. Microw. Theory Techn.*, vol. 64, no. 8, pp. 2519–2528, Aug. 2016.

[22] S. A. Sadrossadat, Y. Cao, and Q.-J. Zhang, "Parametric modeling of microwave passive components using sensitivity-analysis-based adjoint neural-network technique," *IEEE Trans. Microw. Theory Techn.*, vol. 61, no. 5, pp. 1733–1747, May 2013.

[23] H. Ghorbaninejad and R. Heydarian, "New design of waveguide directional coupler using genetic algorithm," *IEEE Microw. Wireless Compon. Lett.*, vol. 26, no. 2, pp. 86–88, Feb. 2016.

[24] D. Plonis, A. Katkevičius, V. Urbanavičius, D. Miniotas, A. Serackis, and A. Gurskas, "Delay Systems Synthesis using Multi-Layer Perceptron Network," *Acta Phys. Pol. A*, vol. 133, no. 5, pp. 1281–1286, May 2018.

[25] D. Plonis, A. Katkevičius, A. Krukonis, V. Šlegerytė, R. Maskeliūnas, and R. Damaševičius, "Predicting the frequency characteristics of hybrid meander systems using a feed-forward backpropagation network," *Electronics*, vol. 8, no. 1, p. 85, Jan. 2019.

[26] J. Cohen, P. Cohen, S. G. West, and L. S. Aiken, *Applied Multiple Regression/Correlation Analysis for the Behavioral Sciences*, 2nd ed., Hillsdale, NJ, USA: Lawrence Erlbaum Associates, 2003.

[27] C.-K. Wei and C.-Z. Ing, "Order selection for same-realization predictions in autoregressive processes," *Ann. Statist.*, vol. 33, no. 5, pp. 2423–2474, 2005, doi: 10.1214/009053605000000525.

[28] M. Hall, G. Holmes, and E. Frank, "Generating rule sets from model trees," in *Proc. 12th Austral. Joint Conf. Artif. Intell.* Sydney, NSW, Australia: Springer-Verlag, 1999, pp. 1–12.

[29] Y. Wang and I. H. Witten, "Induction of model trees for predicting continuous classes," in *Proc. 9th Eur. Conf. Mach. Learn.*, 1997, pp. 1–13.

[30] G. Michel, M. A. Alaoui, A. Lebois, A. Feriani, and M. Felhi, "DVOLVER: Efficient Pareto-optimal neural network architecture search," *CoRR*, vol. 1, pp. 1–13, 2019.
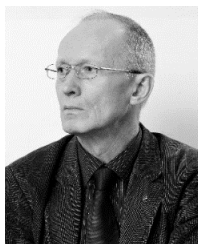
DARIUS PLONIS (Member, IEEE) received the B.S., M.S., and Ph.D. degrees in electrical and electronic engineering from Vilnius Gediminas Technical University, in 2008, 2010, and 2014, respectively. In 2017, he received the title of Associate Professor with VGTU. He is currently an Associate Professor with the Department of Electronic Systems, Vilnius Gediminas Technical University. He has authored more than 30 top research articles. His main research interests include electromagnetic field theory, super-high frequency technologies and microwave devices, signal processing, multimedia, and embedded systems. He is an Active Member of the IEEE Microwave Theory and Techniques. He currently serves as the Secretary for the IEEE Lithuania Section.

ANDRIUS KATKEVIČIUS (Member, IEEE) was born in Vilnius, Lithuania, in 1984. He received the B.S., M.S., and Ph.D. degrees in electrical and electronic engineering from Vilnius Gediminas Technical University, in 2007, 2009, and 2013, respectively. From 2013 to 2019, he was an Associate Professor with the Electronic Faculty, Vilnius Gediminas Technical University (VGTU). He received the title of Associate Professor with VGTU, in 2017. Since 2019, he has been working as a Professor with the Department of Electronic Systems, Electronic Faculty, VGTU. He has authored more than 20 high impact articles. His research interests include high-frequency, microwave and the IoT devices, and embedded systems. He is an Active Member of the IEEE Microwave Theory and Techniques.

ANTANAS GURSKAS was born in Karaganda, Kazakhstan, in 1959. He received the degree in electronics from Kaunas Technology University, in 1982, and the Ph.D. degree in Electrical Engineering from Kaunas Technology University, in 1991. From 1985 to 1991, he was a Researcher and a Lecturer Assistant with Vilnius Gediminas Technical University, where he was a Senior Lecturer from 1991 to 1993 and an Associate Professor from 1991 to 2018. He has authored two monograph books, more than 50 top articles and two inventions. His research interests include mathematical modeling of the planar meander delay lines, algorithms for machinery synthesis of the topology meander delay lines, and advanced measurement systems for the IoT.

VYTAUTAS URBANAVIČIUS (Senior Member, IEEE) was born in Vilnius, Lithuania, in 1956. He received the degree in electrical instrumentation from the Vilnius Electromechanical College, in 1975, the Engineering Diploma degree (Hons.) in electrical and electronics engineering from Vilnius Gediminas Technical University, in 1985, and the Ph.D. degree in electrical and electronics engineering from Vilnius Gediminas Technical University, in 1996. He performed the habilitation procedure at Vilnius Gediminas Technical University, in 2009. From 1975 to 1980, he was an Assistant Lead Engineer with Vilnius Semiconductor Company VENTA. Since 1983, he has been holding various top positions at Vilnius Gediminas Technical University, starting with Research Engineer. Since 2009, he has been a Professor with the Department of Electronic Systems, Vilnius Gediminas Technical University. He has authored of five monograph books, more than 50 major articles, and four inventions. His research interests include microwave delay systems, equivalent time sampling converters, and methods for measuring long-wave electromagnetic radiation in the near field IoT.

RYTIS MASKELIŪNAS received the Ph.D. degree in computer science from the Kaunas University of Technology, in 2009. He is currently a Professor with the Faculty of Informatics, Department of Multimedia Engineering, and also a Chief Researcher with the Centre of Real Time Computer Systems, Kaunas University of Technology. He has authored or coauthored more than 80 refereed scientific articles. His main areas of scientific research are multimodal signal processing, modeling, development and analysis of associative, multimodal interfaces, mainly targeted at elderly and people with major disabilities, also technologies for the development of HCI techniques for patients of Huntington's disease. His main academic subjects are related to computer gaming, development, modeling of mechanics, design and gamification, application design for smart devices, development of user interfaces and usability, development of shaders for 3D graphics, signal processing, and IT project management. He received various awards/honors including the National Science Academy Award for Young Scholars of Lithuania, in 2010, the Best Young Scientist Award of 2012, and others. He serves as a Project Evaluation Expert for multiple scientific organizations, as a Consultant for Eureka and Eurostars calls, and as a Reviewer/Committee Member for various refereed journals.

ROBERTAS DAMAŠEVIČIUS received the Ph.D. degree in informatics engineering from the Kaunas University of Technology (KTU), Lithuania, in 2005. He is currently a Professor with the Software Engineering Department, KTU, and also an Adjunct with the Faculty of Applied Mathematics, Silesian University of Technology, Poland. He has authored more than 250 articles and two monographs published by Springer. His research interests include sustainable software engineering, human–computer interfaces, assisted living, data mining, and machine learning. He is also the Editor-in-Chief of the *Information Technology and Control* journal and has been a Guest Editor of several invited issues of international journals, IEEE Access, *Biomed Research International*, *Computational Intelligence and Neuroscience*, and *Electronics*.

• • •